Thermal convection in monodisperse and bidisperse granular gases: A simulation study

Daniela Paolotti,[1] Alain Barrat,[2] Umberto Marini Bettolo Marconi,[1] and Andrea Puglisi[3]
[1]*Dipartimento di Fisica, Universitá di Camerino and Istituto Nazionale di Fisica della Materia, Via Madonna delle Carceri, 62032 Camerino, Italy*
[2]*Laboratoire de Physique Théorique, Unité Mixte de Recherche UMR 8627, Bâtiment 210, Université de Paris-Sud, 91405 Orsay Cedex, France*
[3]*University "La Sapienza," Physics Department and INFM Center for Statistical Mechanics and Complexity (SMC), Piazzale Aldo Moro 2, 00185 Rome, Italy*
(Received 12 November 2003; revised manuscript received 18 February 2004; published 15 June 2004)

We present results of a simulation study of inelastic hard disks vibrated in a vertical container. An event-driven molecular dynamics method is developed for studying the onset of convection. Varying the relevant parameters (inelasticity, number of layers at rest, intensity of the gravity) we are able to obtain a qualitative agreement of our results with recent hydrodynamical predictions. Increasing the inelasticity, a first continuous transition from the absence of convection to one convective roll is observed, followed by a discontinuous transition to two convective rolls, with hysteretic behavior. At fixed inelasticity and increasing gravity, a transition from no convection to one roll can be evidenced. If the gravity is further increased, the roll is eventually suppressed. Increasing the number of monolayers the system eventually localizes mostly at the bottom of the box: in this case multiple convective rolls as well as surface waves appear. We analyze the density and temperature fields and study the existence of symmetry breaking in these fields in the direction perpendicular to the injection of energy. We also study a binary mixture of grains with different properties (inelasticity or diameters). The effect of changing the properties of one of the components is analyzed, together with density, temperature, and temperature ratio fields. Finally, the presence of a low fraction of quasielastic impurities is shown to determine a sharp transition between convective and nonconvective steady states.

DOI: 10.1103/PhysRevE.69.061304 PACS number(s): 45.70.Qj, 47.27.Te

I. INTRODUCTION

During the last two decades there has been an upsurge of interest for the physical mechanisms which control the behavior of granular media, i.e., systems consisting of a large number of macroscopic grains, such as sand, cereals, powders, etc. [1]. These materials play an important role in many industrial and technological processes and in natural phenomena and their handling has developed into a multibillion-dollar industry. Much experimental and theoretical effort has been spent on understanding their behavior under a variety of conditions. Among the most frequently studied systems are the so called granular gases [2], obtained by subjecting to an external driving force an assembly of grains, so that their behavior resembles that of a molecular gas. However, important differences between the microworld and the macroworld, i.e., between the atomic scale and the millimeter scale, render the analogy incomplete, so that one cannot infer their properties from the knowledge of the molecular level. This irreducibility stems chiefly from the presence of nonconserving forces. Striking manifestations of the peculiarity of granular gases are the non-Maxwellian velocity distributions, the shear instability, the cluster formation to mention just a few.

A typical experiment aimed to probe the behavior of granular gases consists of a vertical container partially filled with spherical particles which are accelerated by a vertically vibrating base [3]. The competition between the dissipation of kinetic energy, due to inelastic collisions between the grains, and the energy provided by the external driving force may lead the system to exhibit a variety of nonequilibrium statistically steady states. The phenomenology resulting from such a simple experimental setup is incredibly rich and by no means trivial. In addition, by varying the control parameters, such as the number of particles, the driving frequency and amplitude, the container aspect ratio, one can observe the crossover from one dynamical phase to another. The exploration of the resulting phase diagram has been conducted by means of laboratory experiments and numerical simulations. Several properties have also been obtained by granular hydrodynamics and kinetic theory. However, such calculations are difficult as the walls and the moving base of the container together with the gravitational field break the translational invariance of the system. As a result, one observes density and temperature gradients which render the theoretical analysis highly nontrivial. In addition, the description of the boundary layers is out of the range of applicability of hydrodynamics.

In the present work we shall focus on the thermal convection instability in granular systems [4–9], which consists in the appearance of convection rolls due to the competition between temperature gradients and gravity. It appears to be different from standard convection, which is induced by boundaries and excluded volume effects [3,11]. Thermal convection in granular media has been first observed in two-dimensional (2D) simulations [4], confirmed by 3D experiments [5], and analytically investigated in Refs. [8,9]. Some numerical investigations can also be found in Refs. [6,7]. The underlying mechanism is analogous to Rayleigh-Bènard convection in classical fluids [10], with the remarkable difference that in a vibrofluidized granular medium the required temperature gradient sets in spontaneously as a consequence

of the interplay between the collisional dissipation of energy in the bulk of the granular gas and of the power injected by the vibrating base.

Hereafter, we shall consider the onset of convective rolls in monodisperse and bidisperse two-dimensional vibrated granular gases and its similarity with the corresponding phenomenon in ordinary fluids. In particular, we shall investigate, by means of event-driven molecular dynamics simulations, a series of predictions provided by the linear stability analysis of hydrodynamic equations [9] for pure granular materials. We shall address the limits of very low and very high intensity of the gravity. In addition, we shall explore the effects of polydispersity on thermal convection, studying a binary mixture of granular gases [12–22,25] with different mechanical properties (in particular, different coefficients of restitution). We shall characterize the standard hydrodynamic fields, namely, velocity, density, and temperature, both in the presence and in the absence of convective rolls.

In Sec. II we define the model employed to simulate the grains in the vibrated container, discuss the relevant dimensionless control parameter, and recall the hydrodynamic predictions. In Sec. III we investigate the pure system and propose a qualitative comparison with the hydrodynamic predictions [8,9] at high and low intensity of the gravity. In Sec. IV we study the binary mixture case, measuring velocity, density, and temperature fields. In Sec. V we study the effect of gradually adding a quasielastic component to a monodisperse system composed of inelastic disks. We observe a sharp transition between a convective and a nonconvective regime. Finally in Sec. VI we present a brief discussion and the conclusions.

II. THE MODEL

Let us consider an assembly of grains constrained to move on a vertical rectangular domain, representing the container, of dimensions $L_x \times L_z$, and subjected to a gravitational force acting along the negative z direction. The grains are idealized as inelastic hard disks of diameter σ and are fluidized by the movement of the base, which oscillates with frequency $\nu=\omega/2\pi$ and amplitude A. The collisions of the particles with the side and top walls conserve their kinetic energy since the latter are immobile, smooth, and perfectly elastic. Instead, the collisions between grains are inelastic, and will be represented by means of nonconstant coefficients of restitution α_{ij}, which are functions of the precollisional relative velocity along the direction joining the centers of a pair, V_n, according to the formula

$$\alpha_{ij}(V_n) = \begin{cases} 1-(1-r_{ij})\left(\dfrac{|V_n|}{v_0}\right)^{3/4} & \text{for} \quad V_n < v_0 \\ r_{ij} & \text{for} \quad V_n > v_0, \end{cases}$$

where i and j indicate the species of the colliding particles, r_{ij} are constants related to the three types of colliding pairs, $v_0=\sqrt{g\sigma}$, and g is the gravitational acceleration. At large relative velocities the functions α_{ij} assume constant values r_{ij}, representing the coefficients of restitution, but tend to the elastic value $\alpha_{ij}(0)=1$ for collisions occurring with vanishing relative velocity. We have checked the insensitivity of our results on the choice of the value of v_0. The use of velocity dependent coefficients of restitution has the merit of avoiding anomalous sequences of collisions among "collapsed" particles [26]. All the lengths are measured in terms of σ.

The full dynamics consists of a succession of free streaming trajectories, which in the presence of the gravitational field have parabolic shapes, and interparticle collisions or wall-particle collisions. It is therefore very convenient to employ the event-driven molecular dynamics. We used the same simulation code of Ref. [25].

The domain was divided into cells and in each cell time-averaged quantities were computed in order to measure the hydrodynamic fields. In such a coarse-grained description we studied the density $\rho(x,z)$ and velocity field $\overline{v}(x,z)$. The local fluctuation of the velocity defines the granular temperature in the cell $\mathcal{C}_{x,z}$ centered around the point of coordinates (x,z):

$$T(x,z) = \frac{m}{2}\langle|\mathbf{v}-\langle\mathbf{v}\rangle_{\mathcal{C}_{x,z}}|^2\rangle_{\mathcal{C}_{x,z}},$$

where the symbol $\langle\cdot\rangle_{\mathcal{C}_{x,z}}$ is an average performed in the cell $\mathcal{C}_{x,z}$. In the measurement procedure we discarded an initial transient and focused on steady state properties.

From the analysis of the time-averaged velocity field we identified the convection rolls without ambiguity by measuring the circulation Φ of the velocity field [4]:

$$\Phi = \frac{1}{N_{paths}}\sum_R \frac{1}{L(C(R))}\oint_{C(R)}\mathbf{v}\cdot d\mathbf{l}. \tag{1}$$

The value of Φ is obtained, in a steady state, by calculating the sum of the integrals along N_{paths} different circular paths $C(R)$ of radius R and of length $L(C(R))$ around the center of the box. The circulation vanishes in the absence of convection or in the presence of an even number of convection rolls, and is finite for an odd number of rolls.

To characterize the dynamical states of the system, it is convenient to introduce three relevant dimensionless parameters [8,9].

The first parameter is the Froude number, which quantifies the relative importance of the potential energy due to the gravity with respect to the energy input at the base. In many previous numerical studies [4,6], the base is "thermal": a particle colliding with the base is reinjected with a velocity taken from a Gaussian distribution of given temperature T_{base}, and thus the Froude number is given by $F_r = mgL_z/T_{base}$. In hydrodynamical studies [8,9], the temperature at the base, T_0, is a boundary condition and $F_r = mgL_z/T_0$. In our model, the base is really vibrating, and the energy received on average by a colliding particle is $mA^2\omega^2$, so that we can choose as definition for F_r,

$$F_r = \frac{2gL_z}{A^2\omega^2} = \frac{L_z}{z_{max}}, \tag{2}$$

where $z_{max}=A^2\omega^2/2g$ is the maximum height reached by a projectile launched vertically with initial velocity $v_0=A\omega$. It is worth to comment that F_r is employed in the present analysis instead of $\Gamma=A\omega^2/g$, which represents the ratio be-

tween the acceleration transmitted by the vibrating wall and the gravitational acceleration. In the case of a vibrating base, we note that, in contrast with the less realistic case of a thermal wall [4,6] which has been used in previous simulations, the mass of the particles does not appear in the definition of the Froude number; this is a relevant point when studying mixtures since different masses do not lead to different Froude numbers. Moreover, the presence of a realistic vibrating wall, instead of a stochastic hot wall (which are not equivalent, see, e.g., Ref. [23]), represents a more severe test of the conjectured convective scenario. In particular, one can answer the question whether the movement of the base breaks the structures and the correlations, and renders the convective rolls unstable.

The second dimensionless parameter relevant for the problem, the Knudsen number [8,9]

$$K = \frac{2}{\sqrt{\pi}}(\sigma L_z \langle n \rangle)^{-1} = \frac{2}{\sqrt{\pi} N_{layers}} \tag{3}$$

is related to the mean free path and $N_{layers} = N\sigma/L$ is the number of filled layers at rest. Finally, in the case of pure (monodisperse) systems, we consider the dissipative parameter

$$R = 8qK^{-2} = \pi(1-r)N_{layers}^2, \tag{4}$$

where $q = (1-r)/2$ is a measure of the inelasticity of the system and r is the coefficient of restitution. R depends both on the inelasticity and on the collision rate, since $R \to 0$ if either $r \to 1$ or $N_{layers} \to 0$.

It is useful to recall the hydrodynamic predictions concerning the phase behavior of the system. In Refs. [8,9] it has been presented the following phase diagram (see Fig. 1): at fixed F_r and K, convection rolls appear with increasing inelasticity, i.e., if R overcomes a critical value R_c. Such a value, R_c, is an increasing function of the Knudsen number K, which in turn decreases with the number of particles present in the system. With respect to the Froude number, instead R_c is a nonmonotonic function of F_r. As shown in Fig. 1, at low F_r (i.e., at low gravity or strong shaking), R_c first decreases, i.e., convection is easier to obtain as the gravity increases. R_c however reaches a minimum and then *increases* as the gravity is further increased. In the following section we show the main results of numerical simulations, observing good *qualitative* agreement with predictions from hydrodynamics; however, since vibrating and thermal walls can yield different behavior for the same value of the parameters [6], no quantitative test will be made.

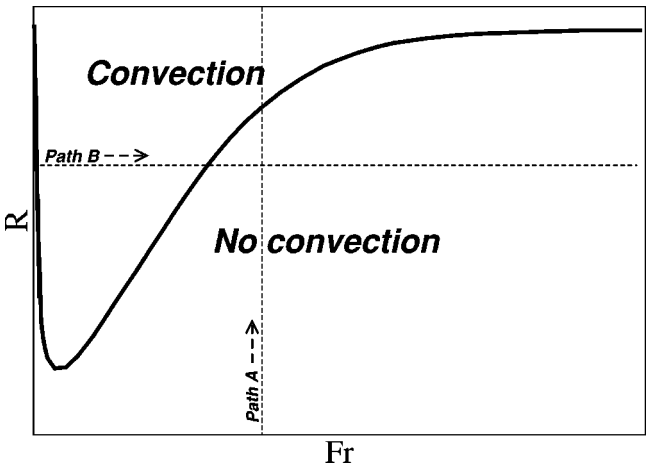

FIG. 1. Phase diagram in the plane (F_r, R), at fixed K, showing the predictions of hydrodynamic theories [8,9]. Convection is expected increasing R, e.g., decreasing the restitution coefficient r, as well as changing F_r in an adequate interval. At too low or too high values of F_r (e.g., very low or very high gravity) the system does not reach convection. The two dashed lines indicate the paths followed in the numerical simulations to verify the predictions. Path A corresponds to Fig. 2, Path B to Fig. 5.

III. CONVECTION IN MONODISPERSE SYSTEMS

We begin by exploring the phase diagram sketched in Fig. 1, obtained from the theory [8,9], along a plane where K is constant and moving along two different paths: a line with constant F_r (path A) and a line with constant R (path B), respectively.

Along path A the effect of increasing R (i.e., of decreasing coefficient of restitution) is to enhance correlations in the system and render steeper and steeper the temperature profile in the vertical direction [9]. This leads to the onset of convection and eventually to the increase of the number of convection rolls. In Fig. 2 we display three pictures corresponding to three different values of R. At $R = 0.64$ one observes the absence of convection, whereas a single roll appears at $R = 32$. Finally two rolls are observed for $R = 159$. The low values of F_r (low gravity) and K (low density) allow the particles to explore the whole box, i.e., regions far from the bottom as well as regions near the base.

Figure 3 displays the evolution of the velocity field circulation during the transient and the stationary regimes in the case of $R = 159$: we see that the system first evolves forming a single convection roll before reaching the stationary state characterized by the presence of two rolls. From Fig. 3 we observe that the formation of a roll occurs sharply.

In Fig. 4 is shown the circulation [defined in Eq. (1)] averaged on times between 300 and 1000 and calculated for different restitution coefficients, between 0.80 and 0.99. This picture illustrates the presence of two transitions, as the restitution coefficient is reduced: there appears to be a continuous transition from absence of convection to one convection roll and a discontinuous transition from one roll to two rolls. This second transition shows hysteresis: the solid line is obtained performing simulations with an increasing restitution coefficient, i.e., decreasing R, and initializing each run with the last configuration of the previous run. The dashed line is instead obtained decreasing the restitution coefficient (increasing R). The transition point changes between the two procedures. As a matter of fact there is a window of values of R where the system may evolve to one or two rolls, depending on initial conditions. Such a hysteretic behavior has been pointed out in Ref. [24], by means of numerical integration of the equations for granular hydrodynamics.

Along path B (R fixed), instead, the system reveals a nonmonotonic behavior [8,9]. In fact, the convection stems from

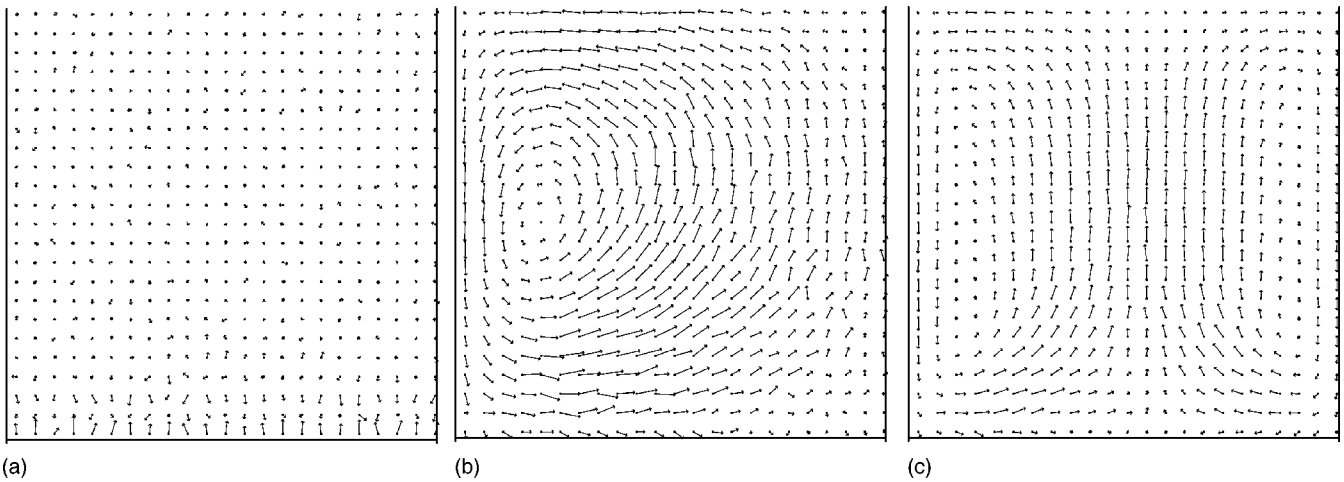

FIG. 2. Pure system: velocity field averaged between $t_1=250$ sec and $t_2=300$ sec, in order to show the onset of convection increasing R, with $F_r=0.36$ and $K=0.071$, $L_x=L_z=113$ cm, $N=1800$, $g=1$ cm/sec^2, $A=0.5$ cm, $\omega=50$ sec^{-1}. From left to right, the three values of restitution coefficient used are $r=0.9992$, $r=0.96$, and $r=0.80$, corresponding to $R=0.64$, $R=32$, and $R=159$, respectively. The length of the arrows is normalized so that the maximum velocity v_{max} observed is represented by an arrow which has a length approximately equal to the distance between two points of the lattice. This convention is used in all figures. In these plots the value of v_{max} is equal to 14.3, 14.5, and 13.6 (in cm/sec) for the case $R=0.64$, $R=32$, and $R=159$, respectively.

the balance between the vertical negative temperature gradients and gravity. Therefore, lowering the intensity of gravity (e.g., inclining the box) reduces such a competition and the value of R_c at which thermal convection can be observed increases. On the other side, when F_r (i.e., gravity) exceeds a certain threshold, there is a crossover to a substantially different regime: the grains tend to remain localized near the vibrating plate. Such a spatial arrangement determines an increase in density in the lower part of the box and tends to inhibit convection, because the packing reduces the mobility of the grains. For this reason when F_r becomes larger, the value of the threshold, R_c, increases. In Fig. 5 such a nonmonotonic behavior is shown: one can see three averaged velocity fields obtained for three different values of F_r, while keeping R and K fixed. To conclude, the patterns obtained by molecular dynamics are consistent with the prediction of Ref. [9] based on granular hydrodynamics.

Next, we have tested the prediction of Ref. [9] regarding the convection at very large values of the Froude number, i.e., when the particles [27] are confined in a region adjacent to the basal plate. In such a case the typical length-scale characterizing the onset of convection suggests the presence

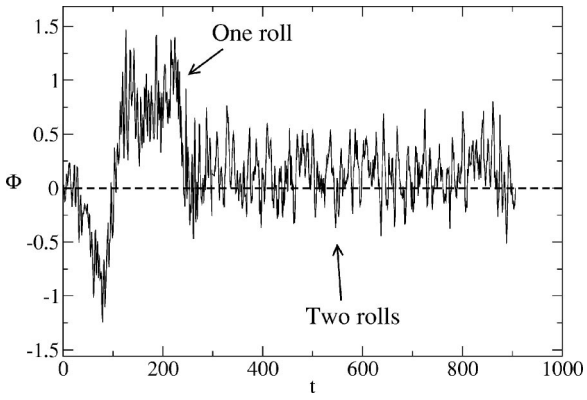

FIG. 3. Pure system: circulation of velocity field Φ (measured in cm/sec) as defined in the text vs time (measured in seconds) for the rightmost system of Fig. 2 (i.e., $F_r=0.36$ and $K=0.071$, $L_x=L_z=113$ cm, $N=1800$, $g=1$ cm/sec^2, $A=0.5$ cm, $\omega=50$ cm^{-1}, $r=0.80$, corresponding to $R=159$). It can be seen that the steady state (identified by $\Phi\simeq 0$, e.g., two opposite convective rolls) is reached after a long transient characterized by nonzero circulation (e.g., an odd number of rolls). In particular, the regime between $t=150$ and $t=250$ sec corresponds to one convection roll very similar to the one depicted in the central frame of Fig. 2, e.g., for a lower value of R.

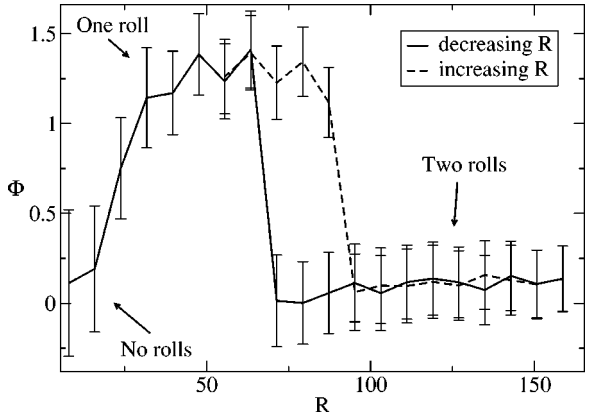

FIG. 4. Pure system: time averages (between time 300 and 1000 sec) of circulation Φ (measured in cm/sec) for different values of restitution coefficient r, i.e. different values of R, with $N=1800$, $L_x=L_y=113$ cm, $K=0.071$, $F_r=0.36$ ($g=1$ cm/sec^2, $A=0.5$ cm, $\omega=50$ sec^{-1}). The solid line is obtained decreasing R and initializing each run with the last configuration of the previous run. The dashed line is obtained with the same procedure but increasing R. The continuous transition from the absence of convection to one convective roll, as well as the discontinuous transition from one roll to two rolls, can be easily recognized. The second transition shows hysteresis.

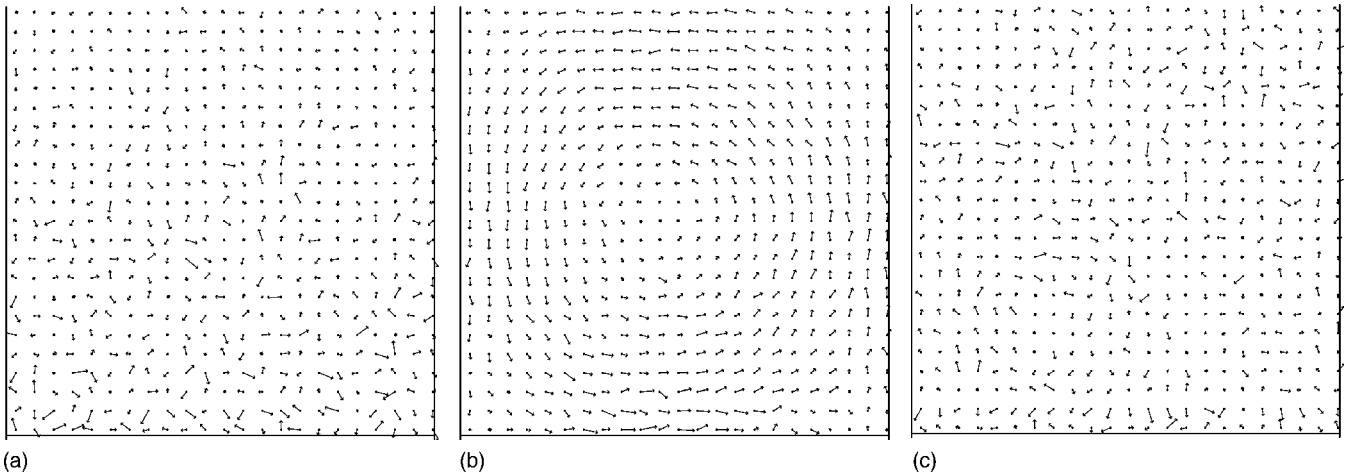

FIG. 5. Pure system: onset and offset of convection (increasing F_r) at $R=3.5$ ($r=0.9955$) and $K=0.07$ fixed, with $L_x=L_z=113$ cm, $N=1800$, $\sigma=1$ cm, $A=0.5$ cm, $\omega=50$ sec^{-1}. The three values of Froude number are, from left to right, $F_r=1$, $F_r=21$, and $F_r=106$, corresponding to $g=3$ cm/sec^2, $g=60$ cm/sec^2, and $g=300$ cm/sec^2, respectively. In correspondence of the lowest value of F_r convection is absent because $R<R_c$, for $F_r=21$ convection appears because $R>R_c$, and finally for $F_r=106$ convection disappears again because $R<R_c$. In these figures the value of v_{max} used to normalize the arrows is 14.3, 4.5, and 2.2 (in cm/sec) for the case $g=3$, $g=60$, and $g=300$, respectively.

of a multiroll configuration. In Fig. 6 we display the velocity field of a system with large aspect ratio $L_x/L_z=1.5$ and a very high Froude number $F_r=22.5$. In this regime, almost no collisions with the upper wall occur, and L_z is therefore essentially irrelevant. Remarkably, five convection rolls are present and a wavelike horizontal profile of the density is observed, revealing a horizontal density instability (see also Ref. [6]). Note that an odd number of rolls can only be obtained with fixed walls boundary conditions, while periodic boundary conditions lead always to an even number of rolls, because neighboring cells must rotate in opposite directions.

In order to complete our description of the hydrodynamic properties of the system, we have analyzed the granular temperature and density fields shown in Fig. 7 (in the case of fixed lateral walls). Both fields show clearly the horizontal inhomogeneity: the density instability and the corresponding temperature instability can be explained in terms of the peculiar clustering mechanism characterizing granular fluids. Inelastic collisions, which occur more frequently in dense regions, determine a reduction of the local temperature and consequently a drop of the local pressure. The ensuing pressure gradient amplifies the density fluctuation and more particles flow toward that region.

Note that the three regions, where the density is larger, are located in correspondence of the three "valleys" at the free surface visible in Fig. 6. The temperature field reflects the symmetries of the density field, and one can see that density and temperature are anticorrelated: the denser regions are colder. For instance, the three "islands" of hot particles correspond to the three lower densities (i.e., the holes left empty by the depression of the free surface, see again Fig. 6). However, above a certain height (about 100), the horizontal instability disappears and both temperature and density decrease together: this is a region with very low number of particles.

Direct comparison between Figs. 6 and 7 clearly shows the strong correlation between the velocity field and the temperature and density fields. In the region separating two convective rolls, two opposite phenomena can be observed: (i) if the velocity field is directed upward, i.e., toward the free surface, the density is relatively low and one observes a bump on the surface; (ii) if the velocity field is directed downward, the bottom plate confines the particles and one observes both a depression in the surface and a high-density region close to the bottom. Each convection roll therefore displays an asymmetric shape with a high-density region coupled to the downward flow and a low-density region coupled to the upward flow. We notice that this phenomenology is slightly different from that observed in Ref. [6], where a convective regime and a clustering regime were studied separately: our simulations indicate a strong interplay between density and velocity fields.

IV. BINARY MIXTURES

In the present section, we shall consider how the convective properties of a granular fluid can be modified by the addition of a second species with different physical properties. First, we shall trigger the convection by tuning the parameters of one of the two species, in the case of equal concentrations. We also consider the local density ratio that accounts for segregation.

While nonequipartition can be determined by differences of either of masses, sizes, or inelasticities, we have mentioned in the Introduction that the Froude number does not depend on the masses of the particles when the energy is injected through a vibrating wall. We shall therefore focus on mixtures of beads with different inelasticities or sizes.

We shall begin with a mixture consisting of two kinds of grains with different coefficients of restitution. We denote with r_{11} the coefficient of restitution relative to collisions among particles both belonging to species 1, r_{22} relative to collisions between particles of species 2, and r_{12} relative to

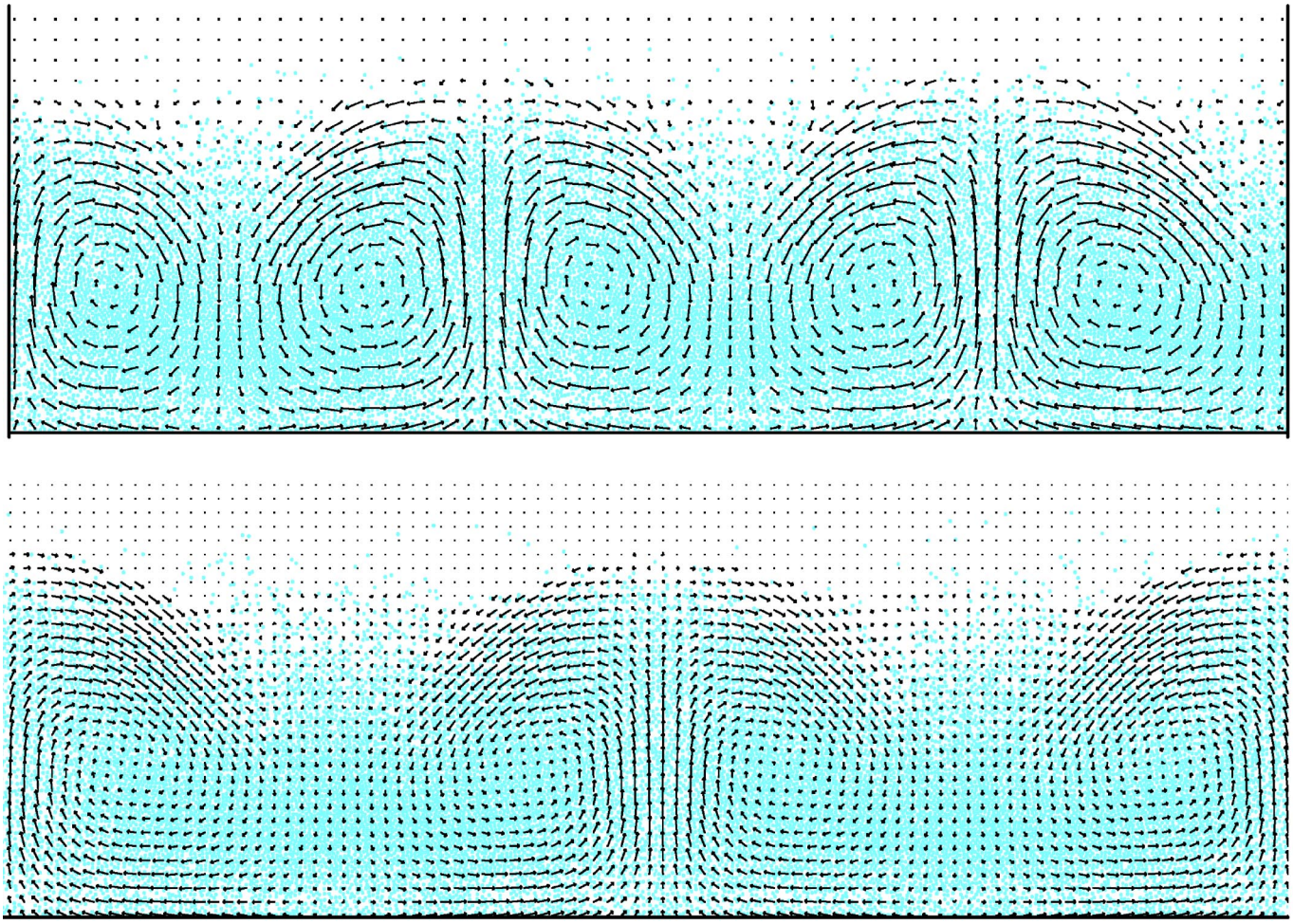

FIG. 6. Pure system: convection at high F_r number (e.g., strong gravity). We used $r=0.991$, $L_x=375$ cm (L_z is irrelevant in this case), $N=18\,000$, $\sigma=1$ cm, $A=0.5$ cm, $\omega=50$ sec^{-1}, $g=28$ cm/sec^2, so that $K=0.023$ and $R=65$. Top—fixed walls boundary conditions; bottom—periodic boundary conditions.

collisions between unlike species. For the sake of simplicity, we shall assume $r_{12}=(r_{11}+r_{22})/2$. Figure 8 shows how the variation of the inelasticity of only one of the two species may change the convective structure: in particular, we reduce r_{22} keeping r_{11} fixed. The species 1 has a restitution coefficient $r_{11}=0.96$ equal to the case of Fig. 2, which displayed a single convection roll. In a first simulation (left frame) the species 2 has a restitution coefficient $r_{22}=0.90$, and still a single convection roll is observed. In a second simulation, with $r_{22}=0.60$, two convection rolls are found. In the same figure we also display two corresponding snapshots, in order to give a hint of the coupling between the rolls and the density: as in the preceding section, regions of high density are coupled to the downward flow of particles. Moreover the snapshots suggest the absence of segregation, as expected for dilute systems. The absence of segregation and the visual inspection of convection rolls suggest a first simple hypothesis for the behavior of a binary mixture with different restitution coefficients: an equimolar mixture behaves similar to a pure gas with an effective restitution coefficient that is roughly an average between those of the two components. In fact in the first case the "average" restitution coefficient is still near the value where a single cell was observed in the pure gas, while in the second case this effective coefficient (around 0.78) is similar to the one corresponding to two rolls in the pure gas (rightmost frame of Fig. 2).

As far as the temperature ratio field T_1/T_2 is concerned, we cannot present a conclusive picture. In fact, the temperature ratio profiles that can be efficiently measured in situations where the systems are horizontally homogeneous (see, for instance, Refs. [13,17,25]) become extremely noisy due to the presence of transversal structures and convection. Our results suggest that the temperature ratio is not appreciably affected by convection rolls or at least the variation with respect to the case without rolls cannot be resolved due to the statistical uncertainty. We recall that in granular gases the breakdown of equipartition is not necessarily related to segregation and can be predicted on the basis of the homogeneous Boltzmann equation for dissipative hard spheres (or disks), both in the absence and in the presence of external driving forces.

Finally, we have studied how to enhance segregation of a mixture, in a case where the global density was higher and the sizes of the particles were different. In particular, we have chosen the parameters corresponding to Fig. 6, but substituted half of the grains with grains having larger diameter

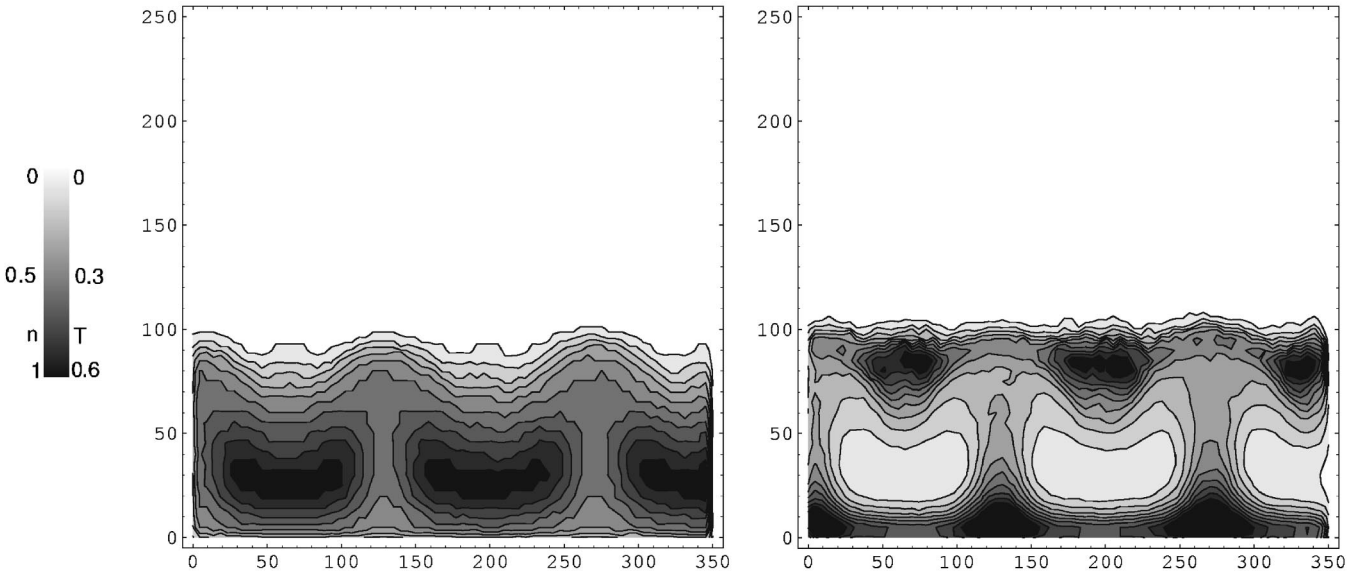

FIG. 7. Pure system: convection at high F_r number (strong gravity), with the same parameters of Fig. 6 (with fixed wall boundary conditions): the density (left) and temperature (right) fields are in arbitrary units.

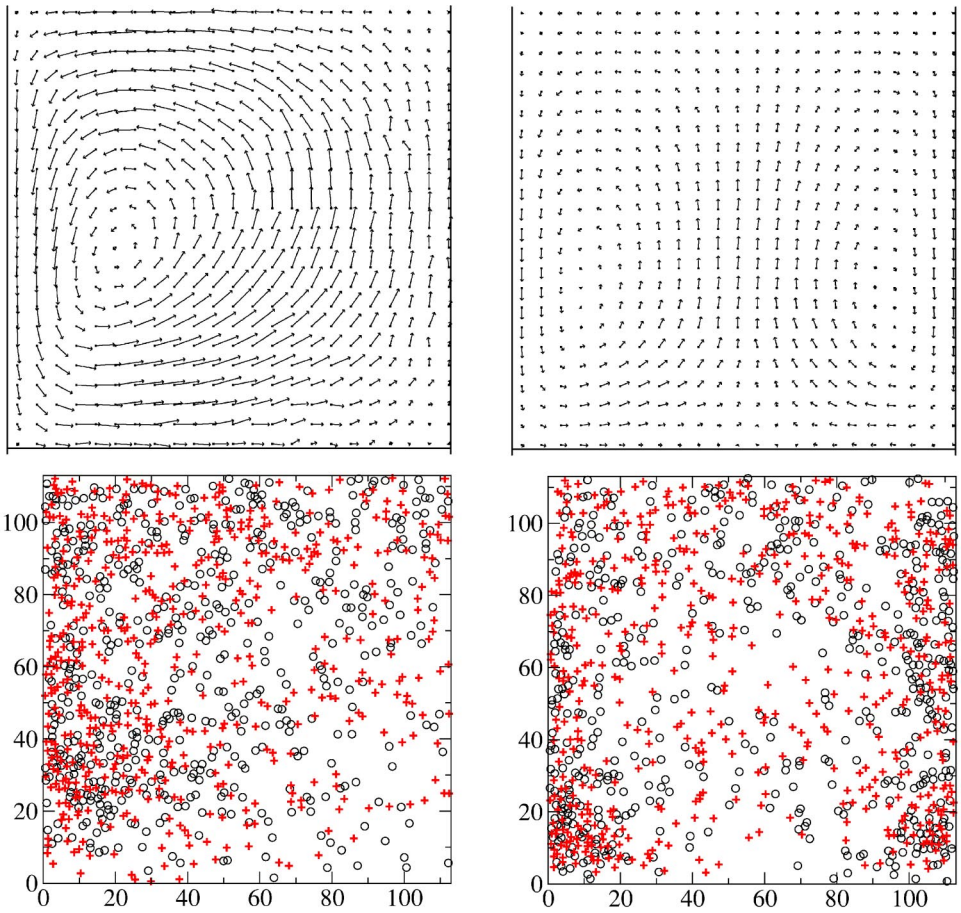

FIG. 8. (Color online) Binary mixture: two different choices of r_{22} determine one or two convective cells; (above) the velocity field, (bottom) a snapshot of particles positions (red crosses and black circles are species 1 and 2, respectively). The parameters used are the following: $\sigma=1$ cm, $L_x=L_z=113$ cm, $N_1=N_2=550$, $g=1$ cm/sec^2, $A=0.5$ cm, $\omega=50$ cm^{-1}, $r_{11}=0.96$, so that $K=0.12$ and $F_r=0.36$. The two values used for r_{22} are 0.90 (left) and 0.60 (right). In the two upper plots the value v_{max} used to normalize the arrows is 9.5 and 7.2 (in cm/sec) for the left and the right case, respectively.

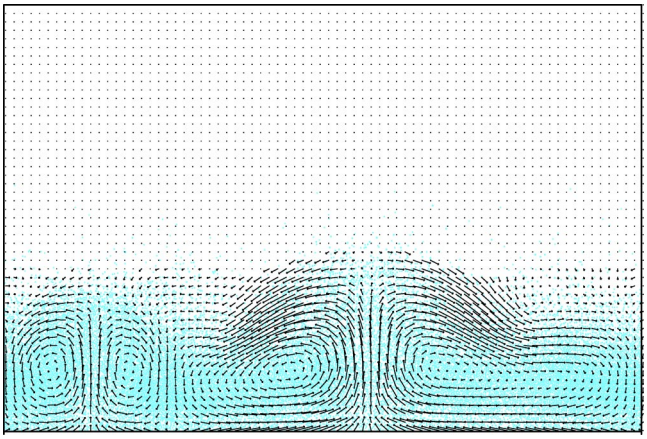

FIG. 9. Binary mixture: a mixture of two different sizes ($\sigma_2/\sigma_1=0.8$ not far from 1) shows differences in the convective pattern, with respect to Fig. 6. The parameters are the same used for that figure. In this plot the value v_{max} used to normalize the arrows is 7.3 cm/sec.

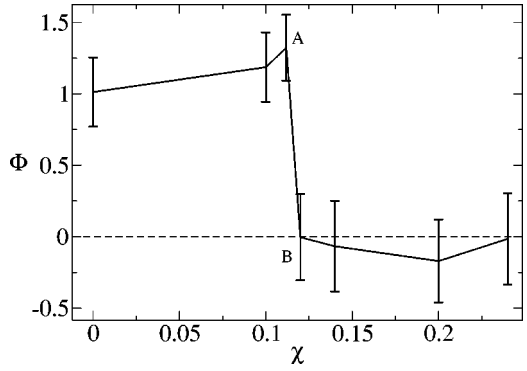

FIG. 11. Averaged circulation ϕ (measured in cm/sec) in a mixture with $L_x=L_y=113$ cm, $g=1$ cm/sec^2, $r_{11}=0.96$, $r_{22}=0.9992$, $N_1+N_2=2200$, corresponding to $K=0.06$, $F_r=0.36$. Doping is measured as percentage of quasielastic particles, i.e., $N_2/(N_1+N_2)$.

$(\sigma_2/\sigma_1=0.8)$. The velocity field is shown in Fig. 9. The field is averaged over very long times, i.e., few hundreds of oscillations of the plate, and the horizontal asymmetry observed appears to be stationary, although, in principle, this pattern is expected to be metastable, in the sense that an infinitely long average should produce a horizontally periodic field. Therefore, a slight change in the size of half of the particles affects the convective field leaving unaltered the number of rolls, but changing their relative size and shape. We have analyzed the density fields of the single species n_1 and n_2 and the density ratio $\gamma=n_2/n_1$, obtaining the results in Fig. 10. Segregation is now evident, appearing as deviations of γ from 1. In particular, it can be noted that at the bottom there are more particles of species 1 (the larger particles). These results call for new experiments in this dilute "granular gas" regime: in fact it is opposite to well known experimental findings in the densely packed regime [3]. Moreover, it appears that stronger segregation is localized in regions of high density.

V. NONEQUIMOLAR MIXTURE

Even in a granular mixture the relative concentration, $\chi=N_2/(N_1+N_2)$, is expected to play an important role. Not only it affects the ratio of the partial granular temperatures, but also can induce a transition from a homogeneous to a convective velocity regime. This has particular relevance, for instance, in industrial processes that require the absence or the presence of convection: in the simulations of this section we show how a small percentage of "doping" quasielastic particles added to an assembly of more inelastic particles can totally suppress convection. By employing as an order parameter to detect the transition the circulation Φ, of the velocity field, already defined in Eq. (1) and varying χ we obtained the curve depicted in Fig. 11. In these simulations, we assumed $r_{11}=0.96$, $r_{22}=0.9992$, $N=N_1+N_2=2200$, K

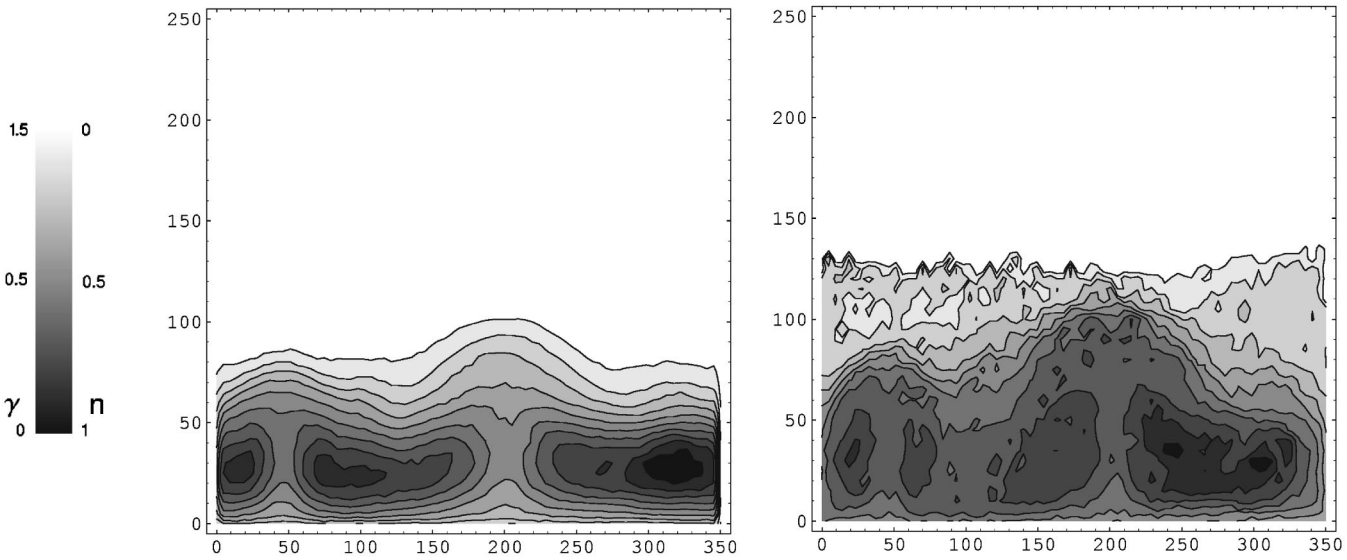

FIG. 10. Binary mixture: Density fields (in arbitrary units); left n_1 field and right ratio $\gamma=n_2/n_1$, with the parameters of Fig. 9.

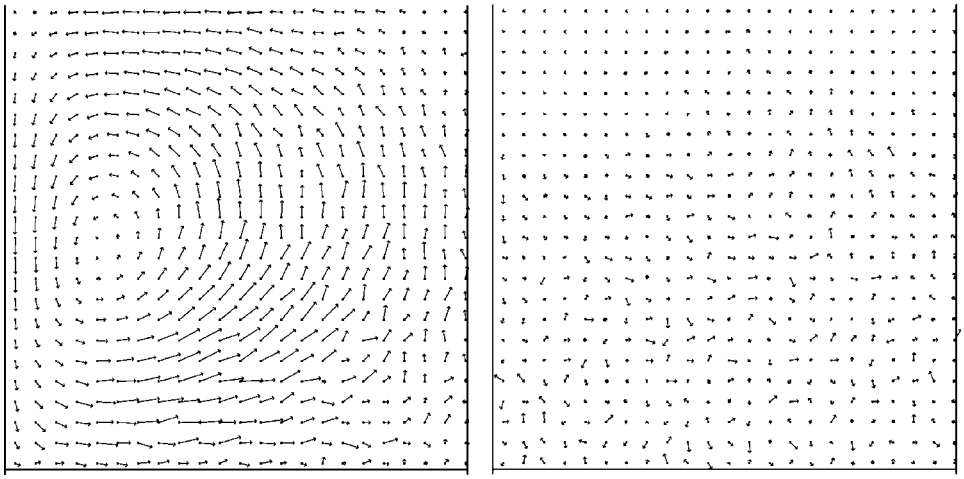

FIG. 12. Averaged velocity field (between $t_1=250$ and $t_2=300$ sec) in a mixture with $L_x=L_y=113$ cm, $g=1$ cm/sec^2, $r_{11}=0.96$, $r_{22}=0.9992$, $N=2200$, corresponding to $K=0.06$, $F_r=0.36$. Left frame corresponds to the point A in Fig. 11 (a doping value $\chi=0.11$), while right frame refers to point B ($\chi=0.12$).

$=0.06$, $F_r=0.36$. While the pure system is in a convective regime, a small doping (the critical value is estimated to be $\chi_{cr}\approx 0.12$) suppresses convection. This critical value changes if the relevant parameters of the system (e.g., K or F_r) are changed. For example, we have verified that increasing F_r the value χ_{cr} increases.

In Fig. 12 we show two different velocity fields observed below and above the critical value of the doping. It is quite striking to observe how the system behavior changes qualitatively in correspondence of a tiny variation of the doping parameter. The simple picture of an effective restitution coefficient (which in this case should be a weighted average between the two coefficients, using the relative compositions as weights) could be an interpretation of the results, as in the preceding section. The transition observed in Fig. 11 could be explained as a transition driven by the effective restitution coefficient when the weights are changed. However the validation of such a hypothesis would require systematic measurements, beyond the aim of the present investigation.

To conclude, we have explored the possibility of a hysteretic behavior: the system has been prepared with a doping value χ slightly higher than χ_{cr}, but with an initial velocity field corresponding to the convective cell at $\chi<\chi_{cr}$. We have studied the temporal evolution of the circulation $\Phi(t)$: the circulation has initially a finite value, but quickly decays to zero, indicating that the convection is rapidly washed out. This behavior excludes therefore the possibility of hysteresis or long transients.

VI. CONCLUSIONS

In this paper, we have studied a two-dimensional granular gas by means of event-driven numerical simulation. We employed a realistic model regarding both the description of the grains as inelastic hard disks and their interactions with the lateral walls and the horizontally oscillating base. The present results are in good qualitative agreement with those predicted by the hydrodynamic theory [8,9]. In particular, we observe the same predicted dynamical regimes and confirm the nontrivial shape of the phase diagram of Ref. [9], where the effects of inelasticity, number of monolayers, and gravity together influence the appearance or disappearance of convection rolls. Within the convective regime, the coupling between the various fields (velocity field, density, and granular temperature) have been characterized. Besides, we have considered the influence of the bidispersity in composition by studying mixtures with different types of grains. This is important in industrial applications, where monodispersity is always difficult to be obtained. We found that the addition of a small fraction of quasielastic component is able to determine the disappearance of the convective rolls. Our results suggest that a granular binary mixture of grains with different inelasticities behaves, from the point of view of convection, as a monodisperse system with an effective restitution coefficient which is roughly the average (weighted with the composition fractions of the two species) of the coefficients of the components. Further investigations are necessary to make this statement more precise.

ACKNOWLEDGMENTS

The numerical code used in the present work was developed by Dr. Ciro Cattuto. We wish to thank him for supporting the simulation work.

[1] H. M. Jaeger and S. R. Nagel, Science **255**, 1523 (1992); H. M. Jaeger, S. R. Nagel, and R. P. Behringer, Phys. Today **49** (4), 32 (1996); Rev. Mod. Phys. **68**, 1259 (1996).
[2] *Granular Gases*, Lectures Notes in Physics Vol. 564, edited by T. Pöschel and S. Luding (Springer-Verlag, Berlin, 2001).
[3] J. B. Knight, H. M. Jaeger, and S. R. Nagel, Phys. Rev. Lett. **70**, 3728 (1993).
[4] R. Ramìrez, D. Risso, and P. Cordero, Phys. Rev. Lett. **85**, 1230 (2000).
[5] R. D. Wildman, J. M. Huntley, and D. J. Parker, Phys. Rev. Lett. **86**, 3304 (2001).
[6] P. Sunthar and V. Kumaran, Phys. Rev. E **64**, 041303 (2001).
[7] J. Talbot and P. Viot, Phys. Rev. Lett. **89**, 064301 (2002); Physica A **317**, 672 (2002).
[8] X. He, B. Meerson, and G. Doolen, Phys. Rev. E **65**, 030301(R) (2002).
[9] E. Khain and B. Meerson, Phys. Rev. E **67**, 021306 (2003).
[10] S. Chandrasekhar, *Hydrodynamic and Hydromagnetic Stability* (Dover, New York, 1981).
[11] J. B. Knight, E. E. Ehrichs, V. Yu. Kuperman, J. K. Flint, H. M. Jaeger, and S. R. Nagel, Phys. Rev. E **54**, 5726 (1996).
[12] Y. Limon Duparcmeur, Thèse de l'université de Rennes I, 1996 (unpublished).
[13] K. Feitosa and N. Menon, Phys. Rev. Lett. **88**, 198301 (2002).
[14] W. Losert, D. G. W. Cooper, J. Delour, A. Kudrolli, and J. P. Gollub, Chaos **9**, 682 (1999).
[15] R. D. Wildman and D. J. Parker, Phys. Rev. Lett. **88**, 064301 (2002).
[16] V. Garzó and J. Dufty, Phys. Rev. E **60** 5706 (1999).
[17] A. Barrat and E. Trizac, Granular Matter **4**, 57 (2002).
[18] J. M. Montanero and V. Garzó, Granular Matter **4**, 17 (2002).
[19] R. Clelland and C. M. Hrenya, Phys. Rev. E **65**, 031301 (2002).
[20] U. Marini Bettolo Marconi and A. Puglisi, Phys. Rev. E **65**, 051305 (2002); **66**, 011301 (2002).
[21] R. Pagnani, U. Marini Bettolo Marconi, and A. Puglisi, Phys. Rev. E **66**, 051304 (2002).
[22] A. Barrat and E. Trizac, Phys. Rev. E **66**, 051303 (2002).
[23] R. Soto and M. Malek Mansour, Physica A **327**, 88 (2003).
[24] P. Cordero, R. Ramirez, and D. Risso, Physica A **327**, 82 (2003).
[25] D. Paolotti, C. Cattuto, U. Marini Bettolo Marconi, and A. Puglisi, Granular Matter **5**, 75 (2003).
[26] N. V. Brilliantov, F. Spahn, J. M. Hertzsch, and T. Pöschel, Phys. Rev. E **53**, 5382 (1996).
[27] Hong-qiang Wang, Guo-jun Jin, and Yu-qiang Ma, Phys. Rev. E **68**, 031301 (2003).